

Nuclear acoustic resonance in single-crystal hydrogen-free tantalum*

R. K. Sundfors, T. H. Wang, D. I. Bolef, and Peter A. Fedders

Laboratory for Ultrasonics, Physics Department, Washington University, St. Louis, Missouri 63130

D. G. Westlake

Argonne National Laboratory, Argonne, Illinois 60439

(Received 6 August 1974)

Nuclear-acoustic-resonance studies have been made of single-crystal 99.99% pure tantalum metal from which all hydrogen has been removed (hydrogen concentration much less than 7 at. ppm or 0.04 wt ppm). The shapes and widths of the ^{181}Ta $\Delta m = \pm 1$ and ± 2 absorption lines can be explained as due to quadrupole broadening caused by a random distribution of charged impurities. Unlike hydrogenated Ta, the $\Delta m = \pm 2$ line shape and linewidth for the hydrogen-free specimen are independent of magnet angle and temperature between 78 and 300 K. The measured ^{181}Ta Knight shift is $(1.14 \pm 0.02)\%$ relative to ^{181}Ta in KTaO_3 . The magnitudes and relative signs of the components of the tensor relating electric field gradient to elastic strain are $S_{11} = \pm 26 \times 10^{15}$ statcoulomb cm^{-3} and $S_{44} = \mp 29 \times 10^{15}$ statcoulomb cm^{-3} .

I. INTRODUCTION

Magnetic-resonance experiments in tantalum metal are strongly affected by the large nuclear-electric-quadrupole moment of ^{181}Ta and by the exothermic interaction between Ta and interstitial impurities of hydrogen atoms. Budnick and Bennett¹ were the first to observe the nuclear magnetic resonance (NMR) of ^{181}Ta in thin tantalum-metal foils which had been heated in a vacuum to approximately 2800 K to remove hydrogen. Nuclear acoustic resonance (NAR) has been used by several investigators to study ^{181}Ta in single-crystal tantalum metal with unknown hydrogen concentrations. Gregory and Bommel² reported the first NAR observation of ^{181}Ta and showed that the coupling between nuclear spins and elastic strains was due to the dynamic electric-quadrupole interaction. Smith and Bolef³ and Smith⁴ studied the temperature dependence of the NAR $\Delta m = \pm 2$ line. Leisure, Hsu, and Seiber⁵ investigated the ^{181}Ta NAR $\Delta m = \pm 1$ and $\Delta m = \pm 2$ lines in high magnetic fields in single-crystal Ta with a small hydrogen concentration in the temperature range 4–150 K. We report in this paper the results of NAR measurements on single-crystal tantalum *from which all hydrogen has been removed* (as explained in Sec. II). This work is part of a general study of the Ta-H system using NAR and ultrasonic absorption and dispersion techniques.⁶

In NAR experiments, time-varying elastic strains due to acoustic waves produce time-varying electric-field gradients at nuclear positions. If the nucleus in question possesses a nuclear-electric-quadrupole moment, acoustic energy may be coupled to the nuclear spin system via the dynamic interaction of the quadrupole moment with these time-varying electric-field gradients. This

is the case for ^{181}Ta in tantalum metal. The electric-field gradient is related to the elastic-strain tensor by a tensor of the fourth rank S .⁷ There are, in general, three nonzero components of the S tensor for crystals with cubic symmetry. These components are S_{11} , S_{12} , and S_{44} when S is expressed in Voigt notation. If one makes the additional assumption that the change in electric charge at the nuclear position with strain is zero, it has been shown⁸ that the number of independent S -tensor components is reduced to two, with $S_{12} = -\frac{1}{2}S_{11}$. In the present NAR study of hydrogen-free single-crystal tantalum metal, we report determinations of S_{11} and S_{44} , details of the hydrogen-free ^{181}Ta linewidth and line shape, and a determination of the ^{181}Ta Knight shift.

II. EXPERIMENTAL

A 2-cm-long Ta single crystal with growth axis along a $[110]$ crystal direction, obtained from Metals Research, was spark-erosion cut, chemically etched, ground, and optically polished to give a cylindrical specimen of length 1.17 cm and diameter 1.04 cm. End faces of the cylinder were made flat and parallel to within $1.3 \mu\text{m}$, and were measured (by x-ray-diffraction techniques) to be within $\pm 0.5^\circ$ of (110) crystal planes. Interstitial hydrogen was removed by heating the sample in vacuum of 2×10^{-6} Torr for 10 h at 1070 K, after which it was allowed to cool slowly (100 K/h) in vacuum to room temperature.

The conditions for hydrogen removal were chosen as a result of the following considerations:

(i) The pressure-composition-temperature diagram for the Ta-H system⁹ allows one to ascertain that the equilibrium concentration of hydrogen under these conditions is considerably less than 7

at. ppm (0.04 wt. ppm).

(ii) The diffusivity of hydrogen in Ta is $\approx 10^{-4}$ $\text{cm}^2 \text{sec}^{-1}$ at 1070 K.¹⁰ With such great mobility, the hydrogen concentration should be very near its equilibrium value throughout a cylinder with the sample dimensions after only 1 h.¹¹

(iii) Analyses by vacuum fusion detected no hydrogen in other samples given a similar treatment.

All crystal cutting and grinding was done prior to the hydrogen removal. After dehydrogenation, the sample was kept in a hydrogen-free environment and handled only briefly during transducer bonding and mounting in the NAR low-temperature probe. Data taking began one week after hydrogen removal. We have also conducted NAR studies on this same sample with different known hydrogen concentrations and with all hydrogen removed a second time 12 months after the first investigation. Both studies on dehydrogenated Ta gave the same ^{181}Ta linewidth and line shape which were independent of temperature in the 78–300-K range. Our studies and other reported studies^{3–5} of hydrogenated Ta show definite ^{181}Ta NAR linewidth and line shape changes in the 78–300-K range which must be associated with the presence of hydrogen in Ta.

Acoustic waves were generated by means of AT-cut (transverse) or X-cut (longitudinal) quartz piezoelectric transducers bonded to the specimen with Nonaq stopcock grease. The coaxial cylindrical transducers were 0.953 cm in diameter with a center acoustic radiating area of diameter 0.64 cm. Acoustic properties (mechanical resonance “ Q ” and frequency) of the composite resonator (sample plus bond plus transducer) were measured using a Hewlett-Packard model 250A RX meter. NAR absorption measurements were made at 5 and 10 MHz, utilizing a standard marginal oscillator ultrasonic spectrometer (MOUS).¹² Absolute change in acoustic attenuation was obtained by comparison of the NAR signal amplitude with a calibrator signal.¹² The absorption line was determined by numerically integrating the experimentally observed NAR derivative signal. Maximum signal-to-noise ratio of the $\Delta m = \pm 2$ NAR signal exceeded 100/1; a much poorer signal-to-noise ratio was observed for the $\Delta m = \pm 1$ NAR signal because of the large linewidth.

The technique of NAR measures the acoustic-attenuation change associated with absorption of resonant acoustic energy by a nuclear-spin system.¹³ As noted above, the dominant coupling between the elastic strains and the ^{181}Ta nuclear-spin system is the dynamic-quadrupole interaction. The S-tensor component S_{11} was determined using transverse acoustic waves with propagation vector \vec{k} along [110] and polarization vector $\vec{\xi}$ along $[1\bar{1}0]$. Using the notation of an earlier paper,¹⁴ we write

the attenuation change as

$$\Delta\alpha_{(\Delta m=\pm 2)} = \frac{3}{4} CB_2 (QS_{11} \cos\chi)^2, \quad (1)$$

where χ is the angle in the (110) plane between the external magnet field \vec{H} and [001];

$$B_2 = \sum_m F_m(I)_{\pm 2}^2, \quad F_m(I)_{\pm 2} = [(I \mp m)(I \mp m - 1) \\ \times (I \pm m + 1)(I \pm m + 2)]^{1/2},$$

$$C = \frac{\pi^2}{16(2I)^2 (2I-1)^2 (2I+1)} \frac{N\nu^2 e^2 g(\nu)}{\rho\nu^2 kT},$$

where I is the nuclear spin, N is the number of resonant nuclear spins per unit volume, ν is the acoustic-wave frequency, $g(\nu)$ is the normalized line-shape function, ρ is the mass density, v is the acoustic-wave velocity, k is the Boltzmann constant, and T is the absolute temperature. Similarly, S_{44} was measured by propagating transverse acoustic waves with \vec{k} along [110], $\vec{\xi}$ along [001], and \vec{H} again in the (110) plane. The acoustic-attenuation change for this case is

$$\Delta\alpha_{(\Delta m=\pm 2)} = 4CB_2 (QS_{44} \sin\chi)^2. \quad (2)$$

Relative signs between S_{11} and S_{44} were measured by propagating longitudinal acoustic waves with \vec{k} along [110] and \vec{H} in the (110) plane. The attenuation change for this case is

$$\Delta\alpha_{(\Delta m=\pm 2)} = CB_2 Q^2 \left[\frac{3}{4} S_{11} \sin^2\chi + S_{44} (1 + \cos^2\chi) \right]^2. \quad (3)$$

III. RESULTS AND DISCUSSION

The experimental NAR $\Delta m = \pm 2$ line shape is given in Fig. 1 and the absorption line shape computed from Fig. 1 is shown in Fig. 2. In Fig. 3 we show the $\Delta m = \pm 1$ absorption line shape. The differences in signal-to-noise ratio between Figs. 2 and 3 are caused by (a) much poorer composite resonator acoustic properties at 5 MHz than at

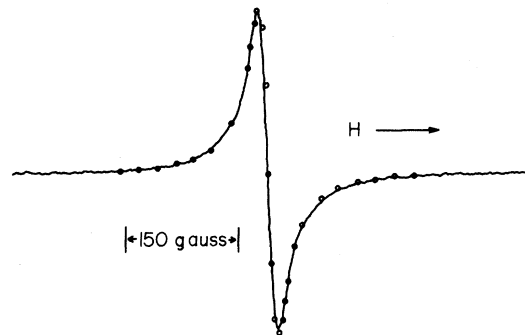


FIG. 1. NAR $\Delta m = \pm 2$ experimental line $\vec{k} \parallel [110]$, $\vec{\xi} \parallel [1\bar{1}0]$, $\chi = 0^\circ$, 10 MHz, 300 K, modulation amplitude 3G. The plotted points are from the theoretical model of a sum of Lorentz line-shape functions.

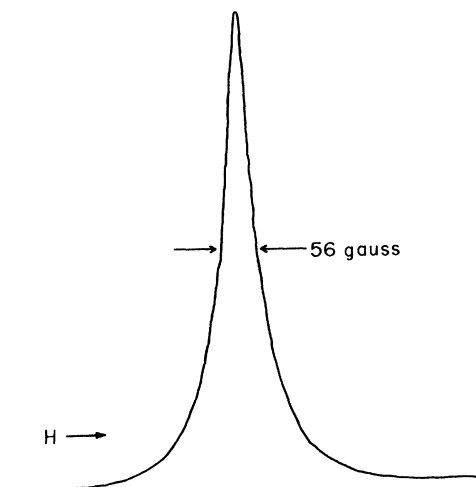


FIG. 2. NAR $\Delta m = \pm 2$ absorption line determined by integrating Fig. 1.

10 MHz and (b) much smaller ratio of modulation-field amplitude to linewidth in Fig. 3 than in Fig. 2.

Experimental NAR changes in attenuation with magnet angle follow the theoretical dependence predicted by Eqs. (1)–(3) at 78 and 300 K. We find no evidence of the anomalous behavior reported in earlier experiments.²

A. Knight shift and S -tensor components

The center of the ^{181}Ta NAR $\Delta m = \pm 2$ experimental resonance line of Fig. 1 corresponds to a magnetic field of 9412 ± 2 G at a frequency of 9.700334 MHz. Relative to the Bennett and Budnick¹⁵ value for ^{181}Ta in KTaO_3 , the shift is determined as $(1.14 \pm 0.02)\%$. Budnick and Bennett¹ measured the Knight shift as 1.1% in Ta metal foils.

From the measured values of $\Delta\alpha$ we obtain, using Eqs. (1)–(3), the products QS_{11} and QS_{44} to within 10%. Using a value¹⁶ of $Q = (3.9 \pm 0.4) \times 10^{-24}$ cm^2 , we determine $S_{11} = \pm 26 \times 10^{15}$ statcoulomb cm^{-3} and $S_{44} = \mp 29 \times 10^{15}$ statcoulomb cm^{-3} .

Electric-field gradients in metals are generally assumed¹⁷ to be due to the sum of lattice and conduction-electron contributions. Buttet¹⁸ has computed the lattice contributions to S_{11} and S_{44} in aluminum on the assumption of a point-charge model for the ion charges at lattice positions. We compute the lattice contributions S_{11}^* and S_{44}^* with the same point-charge assumption and approximate the lattice sum by summing point-charge contributions out to the 25th shell from a nuclear position. This lattice contribution is

$$S_{11}^* = 3.5Z^*e(1 - \gamma_s)d^{-3},$$

where $Z^* = +1$, e is the electron-charge magnitude, d is the first-neighbor distance, and γ_s is the

Sternheimer antishielding factor for the solid. Using $d = 2.86$ Å,¹⁹ we find $1 - \gamma_s = 300$ is required to explain the experimental S_{11} if there is *zero* conduction-electron contribution. The ratio of the lattice contributions $S_{11}^*/S_{44}^* = -2.0$; the measured ratio of $S_{11}/S_{44} = -0.9$. The large value of $(1 - \gamma_s)$ and the difference in these ratios imply a sizeable conduction-electron contribution. Similar differences between measured quadrupole-coupling constants and computed lattice contributions in hexagonal-close-packed large-atomic-number metals have been noted by Das and Pomerantz.²⁰

B. Line shapes

1. $\Delta m = \pm 2$ line

Our studies of the $\Delta m = \pm 2$ NAR show that its line shape and linewidth are independent of temperature in the range 78–300 K and are also independent of magnetic-field orientation for rotations of magnetic field in two different $\{110\}$ planes. As noted in Sec. II, this is in contrast to previous NAR results^{3–5} with hydrogenated single-crystal Ta. In addition, the absorption linewidth from Fig. 2 is 56 G at half-amplitude, which is much greater than the 2.65 G computed¹ for the dipole-dipole linewidth in Ta powder.

We can think of only two mechanisms which are consistent with temperature independence and angular isotropy. They are (i) pseudoexchange between like spins²¹ and/or (ii) static-quadrupole broadening due to electric-field gradients generated by a random distribution of charged defects and impurities screened by spherically symmetric conduction electrons. We wish to point out that field gradients generated by strains cannot lead to a spherically symmetric line shape simply because this would require both the S tensor and the elastic constants to possess spherical symmetry. Spherical symmetry of elastic constants [$c_{11} = c_{44} = \frac{1}{2}(c_{11} - c_{12})$] and of the S -tensor components ($\frac{3}{4}S_{11} = S_{44}$) is broken by more than a factor of 2 in Ta.

The experimental evidence is quite conclusively in favor of the charged-defect mechanism. The strongest evidence is the excellent fit obtained between theory and experiment, using this model, which is shown in Fig. 1. This fit was made using a sum of Lorentzian derivative curves centered about zero with half-widths and weighting factors appropriate for the different $\Delta m = \pm 2$ transitions²¹ possible for a nuclear-spin $I = \frac{7}{2}$ system. The adjustable parameters used were an over-all amplitude factor and a single linewidth factor. A single Lorentzian line does not fit the data. It would be quite a coincidence if the pseudoexchange line shape also fit this well, especially since it is believed to be approximately Gaussian.

In addition, a pseudoexchange mechanism pre-

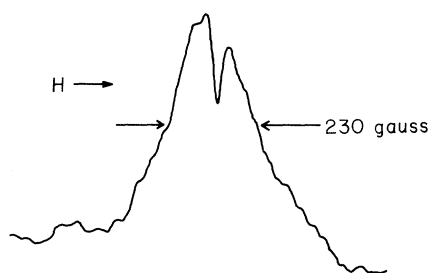


FIG. 3. NAR $\Delta m = \pm 1$ absorption line $\vec{k} \parallel [110]$, $\vec{\xi} \parallel [1\bar{1}0]$, $\chi = 90^\circ$, 5 MHz, 300 K, modulation amplitude 4.7 G.

dicts²¹ that the ratio of the $\Delta m = \pm 1$ linewidth to the $\Delta m = \pm 2$ linewidth is 2. The sum of Lorentzians, on the other hand, predicts that this ratio is 3. To within experimental error, the observed ratio is between 3 and 4.

2. $\Delta m = \pm 1$ line

The line shape of the $\Delta m = \pm 1$ NAR in Fig. 3, including the anomaly, in the center, is also independent of magnetic-field orientation although the signal-to-noise ratio is much poorer than for the $\Delta m = \pm 2$ NAR. This anomaly has been observed in a previous NAR study⁵ of single-crystal Ta with 6.8-ppm hydrogen by weight and interpreted as a splitting due to electric-field gradients which are random in direction but approximately the same magnitude at any ¹⁸¹Ta nuclear position. Their observed $\Delta m = \pm 1$ and $\Delta m = \pm 2$ line shapes at 10 K are similar to those shown in Figs. 1–3. Except for the anomaly in center of the $\Delta m = \pm 1$ NAR line, the line shape is consistent with the discussion of the $\Delta m = \pm 2$ NAR line shape.

In our discussion of the anomaly, several possibilities can be ruled out.

(a) The anomaly cannot be a line splitting due to a net field gradient in the crystal. The existence of such a field gradient implies a unique axis and thus the anomaly should be angle dependent, which it is not. Further, any such net field gradient would also split the $\Delta m = \pm 2$ NAR, and this

effect is not observed. The anomaly also cannot be explained by a random distribution of electric-field gradients at the ¹⁸¹Ta nuclear positions due to charged interstitial impurities or defects. Such a distribution of impurities or defects which are random in direction and in magnitude at the nuclear positions contributes to the line broadening but cannot cause the $\Delta m = \pm 1$ splitting. Finally, the slope of the anomaly is greater than the slope of the outside of the resonance line. This is in contradiction to any observed splitting and any rational theory based on field gradients.

(b) The anomaly is not due to the resonant Alpher-Rubin coupling which sometimes can cause an emissive looking absorption.^{22–25} The magnitude of the resonant Alpher-Rubin coupling vanishes when the magnetic field is perpendicular to the propagation direction. The observed angular dependence of the acoustic attenuation change of the anomaly is totally inconsistent with Alpher-Rubin coupling.

(c) The anomaly is not due to any coupling to external rf fields. This possibility was eliminated by shielding the entire sample, including the area under the transducer, by a grounded copper conductor of one skin depth in thickness.

Such a line shape as in Fig. 3 has been observed in a $\Delta m = \pm 1$ NAR study²⁶ of the semiconductor CuI²⁷. An anomalous line shape similar to Fig. 3 has also been observed in the electron spin resonance of Ni²⁺ in MgO and interpreted²⁷ as due to internal cross relaxation. One of us has recently published²⁸ a theory of the line shape changes due to intraspin cross relaxation. This theory produces qualitatively similar, but as yet not detailed, line shapes similar to Fig. 3. In fact, without intraspin cross relaxation, it is impossible to obtain a split line (or a dip) from a spherically symmetric random field gradient distribution.^{28,29}

ACKNOWLEDGMENT

We thank S. T. Ockers for his invaluable aid in preparing single-crystal Ta with known hydrogen concentrations.

*Work supported in part by the National Science Foundation.

¹J. I. Budnick and L. H. Bennett, *J. Phys. Chem. Solids* **16**, 37 (1960).

²E. H. Gregory and H. E. Bommel, *Phys. Rev. Lett.* **15**, 404 (1965).

³R. E. Smith and D. I. Bolef, *Phys. Rev. Lett.* **22**, 183 (1969).

⁴R. E. Smith, Ph.D. thesis (Washington University, 1969) (unpublished).

⁵R. G. Leisure, D. K. Hsu, and B. A. Seiber, *Phys. Lett. A* **42**, 195 (1972); *J. Appl. Phys.* **44**, 3394 (1973).

⁶T. H. Wang, R. K. Sundfors, and D. I. Bolef, *Bull. Am.*

Phys. Soc. **18**, 95 (1973).

⁷E. F. Taylor and N. Bloembergen, *Phys. Rev.* **113**, 431 (1959).

⁸R. J. Harrison and P. L. Sagalyn, *Phys. Rev.* **128**, 1630 (1962).

⁹E. Veleckis and R. K. Edwards, *J. Phys. Chem.* **73**, 683 (1969).

¹⁰G. Schaumann, J. Völkl, and G. Alefeld, *Phys. Status Solidi* **42**, 401 (1970).

¹¹J. Crank, *The Mathematics of Diffusion* (Clarendon, Oxford, 1956), p. 67.

¹²D. I. Bolef and J. G. Miller, *Physical Acoustic* (Academic, New York, 1971), Vol. 8, Chap. 3.

- ¹³D. I. Bolef, *Physical Acoustics* (Academic, New York, 1966), Vol. 4A, Chap. 3.
- ¹⁴R. K. Sundfors, Phys. Rev. 177, 1221 (1969).
- ¹⁵L. H. Bennett and J. I. Budnick, Bull. Am. Phys. Soc. 4, 417 (1959).
- ¹⁶C. H. Townes, *Handbuch der Physik* (Springer-Verlag, Berlin, 1958), Vol. 38/1, p. 377.
- ¹⁷A. J. Freeman and R. E. Watson, in *Magnetism*, edited by G. T. Rado and H. Suhl (Academic, New York, 1965), Vol. IIa.
- ¹⁸J. Buttet, J. Phys. F 3, 918 (1973).
- ¹⁹F. Ducastelle, R. Caudron, and P. Costa, J. Phys. Chem. Solids 31, 1247 (1970).
- ²⁰T. P. Das and M. Pomerantz, Phys. Rev. 123, 2070 (1961).
- ²¹R. K. Sundfors, Phys. Rev. 185, 458 (1969).
- ²²J. G. Miller, W. D. Smith, D. I. Bolef, and R. K. Sundfors, Phys. Rev. B 3, 1547 (1971).
- ²³P. A. Fedders, Phys. Rev. B 7, 1739 (1973).
- ²⁴J. Buttet, Solid State Commun. 9, 1129 (1971).
- ²⁵R. G. Leisure, D. K. Hsu, and B. A. Seiber, Phys. Rev. Lett. 30, 1326 (1973).
- ²⁶R. K. Sundfors (private communication).
- ²⁷S. R. P. Smith, F. Dravnieks, and J. E. Wertz, Phys. Rev. 178, 471 (1969).
- ²⁸Peter A. Fedders, Phys. Rev. B 11, 995 (1975).
- ²⁹Peter A. Fedders, Phys. Rev. B 11, 1020 (1975).